Increasing the Capacity of Magnetic Induction Communication Using MIMO Coil-Array

Hongzhi Guo and Zhi Sun
State University of New York at Buffalo, Buffalo, NY, USA
{hongzhig, zhisun}@buffalo.edu

***Abstract*—Magnetic Induction (MI) is a promising solution for wireless communications in complex environments, such as oil reservoir, underground, indoor, and underwater. Due to the inherent electrically small size and simple structure of the magnetic coil antenna, it suffers from low radiation efficiency, extremely narrow bandwidth, and dramatic polarization loss. Recently, significant efforts have been made to increase MI communication's performance, for instance, the metamaterial-enhanced magnetic induction has been developed to increase the signal strength, the tri-directional coil antenna is used to overcome the polarization loss, among others. However, increasing the bandwidth of MI communication is still a great challenge. In this paper, we propose a MIMO antenna array with each antenna element having its own resonant frequency. Due to the strong coupling in the deep near field, the antenna elements mutually affect each other. Instead of eliminating this coupling, we rigorously derive a model to capture it and use metamaterial-inspired method to find the optimal configuration of the antenna array to achieve multiple bands. As a result, the overall bandwidth can be significantly increased. Meanwhile, the enhanced wireless channel can provide much better signal strength. Finally, we theoretically analyze the channel gain in comparison with the original MI to demonstrate the benefits of MI MIMO.**

I. Introduction

Magnetic Induction (MI) has been a promising solution for wireless communications in complex environments, such as underground, and underwater [1], [2], [3]. This is due primarily to the long wavelength since its operating frequency is in, or even below, high frequency (3-30 MHz) band. MI communication leverages the near field of the coil antenna to achieve less multipath fading and thus a reliable channel. However, because of the inherent electrically small size and simple structure of the magnetic coil antenna, the original MI communication [1] suffers from low radiation efficiency, dramatic polarization loss, and extremely narrow bandwidth.

Research efforts have been made to address these challenges. First, Metamaterial-enhanced MI (M^2I) has been proposed and theoretically analyzed in [4] to increase the radiation efficiency of MI coil antenna. A practical design prototype is demonstrated in [5] to realize the ideal metamaterial model. In addition, the tri-directional coil antenna is used to overcome the polarization loss and this concept has been experimentally validated in [6].

In spite of the fact that MI communication is becoming more and more efficient, its bandwidth is still extremely small. In order to enlarge its bandwidth, the broadband or multiband coil antenna can be a solution. Nevertheless, the intrinsic resonance of MI coil antenna results in narrow bandwidth and the additional inductance to achieve multiband further reduces its overall bandwidth. Therefore, we cannot rely on the single coil antenna to broad its bandwidth.

By examining the M^2I and tri-directional coil antenna, it is obvious that the coil antenna array has brought many benefits to MI communication. Although the single coil antenna has low efficiency, by adding a passive spherical coil antenna array its efficiency can be significantly increased [5]. Moreover, the single coil antenna has high polarization loss, but using three different polarized coil antennas the loss can be dramatically reduced. With this in mind, we propose to use a MIMO coil antenna array to increase MI communication's bandwidth. Each element in the array is resonant at its own frequency. However, due to the strong near field coupling, the antenna array, as a whole system, has drastically different resonant frequencies from its elements. Hence, it is necessary to capture and design the coupling to let the antenna array operate at the expected frequency bands.

The proposed MI MIMO is different from terrestrial wireless MIMO communication in two aspects. First, terrestrial wireless MIMO system is utilized to obtain more diversities and larger channel capacity. The coupling among antennas can dramatically change the antenna array's diversity [7], [8] and thus it needs to be reduced. In contrast, in this paper MI MIMO is utilized to achieve multiband and the antenna coupling can be involved in the system provided that it can be accurately captured. Second, in terrestrial MIMO, the antenna elements have the same configuration, MI MIMO antennas are designed to be different intentionally to achieve multiple frequency bands. In addition, existing MI MIMO [1], [9] have different objectives from this paper. The MI waveguide in [1] has multiple relaying coil antennas which can enhance the signal strength within very narrow bandwidth; it can be regarded as a distributed M^2I. In [9], although multiple coil antennas are used, the antenna coupling is reduced to make each element independent and the bandwidth is not changed.

In this paper, before diving into the strongly coupled multiple antenna array, a 2 by 2 coil antenna array is analyzed to gain insights. We demonstrate how the two transmitting or receiving antennas can affect each other and the way we can create dual resonant frequencies to enlarge the overall bandwidth. Also, the optimal antenna configuration to obtain the expected frequency bands is rigorously found. After that, we smoothly extend our design to even larger size antenna array. By using the same methodology, we propose an algorithm to achieve resonance at any frequency band. Then, based on the designed antenna array, we evaluate the channel capacity

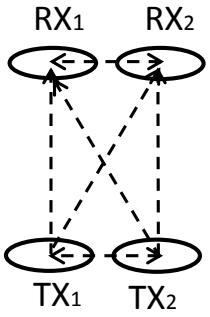

Fig. 1. Illustration of magnetic induction MIMO communication.

by comparing the MI MIMO with the original MI at both high SNR regime and low SRN regime. The developed model shows promising improvement which can not only be utilized in MI communication but also any other deep subwavelength antenna array design.

The reminder of this paper is organized as follows. A dual band 2×2 MI MIMO antenna array is analyzed in detail in Section II. After that, the multiple bands antenna array with arbitrary resonant frequency is designed in Section III. This is followed by the channel capacity analysis in Section IV. Finally, this paper is concluded in Section V.

II. Dual Channel 2×2 MI MIMO

In this section, we first analytically study a 2×2 MI MIMO for the sake of simplicity. The transmitting antenna efficiency and mutual coupling are explicitly derived, upon which we find the resonant condition of the antenna array. After that, we investigate the mutual coupling effect on receiving antenna. Finally, we validate the developed model by using full-wave simulation in COMSOL Multiphysics. The results derived in this section are intended to help us understand the physical philosophy of mutual antenna interaction and provide guidelines for even larger antenna array design.

A. Single Input Transmitting Antenna Array

As shown in Fig. 1, there are 2 transmitting antennas and 2 receiving antennas. Our objective is, from the perspective of the antenna array, TX_1 and TX_2 transmit single at frequency ω_1 and ω_2, respectively, and RX_1 and RX_2 receive signal at frequency ω_1 and ω_2, respectively. In contrast, from the perspective of each antenna, TX_1 and RX_1 should resonant at frequency ω_3, while TX_2 and RX_2 should resonant at frequency ω_4. Note that, $\omega_3 \neq \omega_1$ and $\omega_4 \neq \omega_2$, because the antennas have strong mutual coupling which drives the overall resonant frequency to other frequency bands. Moreover, due to the coupling, antenna's efficiency is also reduced. Nevertheless, in this subsection, we show that the negative effect of mutual coupling can be eliminated provided that we can optimally design the antennas' parameters. Although there are two inputs, we first consider only TX_1 is active, in this way we can investigate the coupling effect of TX_2 on TX_1.

The transmitting antenna's and receiving antenna's equivalent circuits are depicted in Fig. 2. The coil antenna's resistance, self-inductance, series capacitance, source output resistance, load resistance are R_0, L_c, C_a, R_s and R_L, respectively. An impedance transformer is used to match the coil

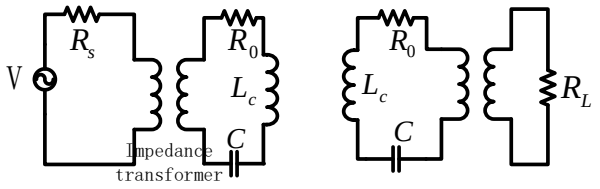

Fig. 2. Equivalent circuit of transmitting and receiving antenna.

antenna with the source or load. In the following, we use R_c to denote the sum of the coil resistance and transformed resistance from the source or the load.

Based on the equivalent circuit we can obtain,

$$TX_1: \ R_c I_1 + jX_1 I_1 + j\omega M I_2 = V \tag{1}$$

$$TX_2: \ R_c I_2 + jX_2 I_2 + j\omega M I_1 = 0, \tag{2}$$

where M is the mutual inductance between the two coils, and $X_i = \omega L_c - \frac{1}{\omega C_i}$. By assuming $X_1 = X_2 = X$, i.e., the two coils are compensated by capacitors with the same value, and adding (1) and (2), this gives

$$R_c(I_1 + I_2) + j(X + \omega M)(I_1 + I_2) = V. \tag{3}$$

In this way, the active coil antenna TX_1 and the passive coil antenna TX_2 described by (3) can be regarded as an equivalent coil whose resistance is R_c, reactance is $X + \omega M$, and current is $(I_1 + I_2)$.

Next, we show that this equivalent coil is more efficient than a single coil, i.e., there is no TX_2. First, in [10], the antenna's radiation efficiency is defined as

$$\eta_1 = \frac{P_{rad}}{P_{rad} + P_{loss}}, \tag{4}$$

where P_{rad} is the radiation power and P_{loss} is the power dissipated on the antenna. However, this efficiency is under the condition that the antenna is well matched, i.e., the reactance is zero. In original MI and M^2I, we matched the transmitting antenna to satisfy this condition. Nevertheless, in MI MIMO, the system is more flexible, in other words the antenna's reactance may not be zero due to mutual coupling. Although, from single antenna's perspective, it's not the optimal condition, but it can achieve the best performance in terms of the antenna array system. Therefore, we consider the antenna can be not well matched and involve the reactance into the antenna efficiency which is

$$\eta_2 = \frac{P_{rad}}{P_i} = \frac{P_{rad}}{P_{rad} + P_{loss} + P_{rac}}, \tag{5}$$

where P_i is the input power and P_{rac} is the power stored in reactive elements.

For a single coil, $R_c I_0 + jX_0 I_0 = V$. Usually, by using a capacitor, X_0 is tuned to be 0. As a result, $I_0 = V/R_c$ and the input power is $P_{i0} = 1/2|I_0 V|$. Analogous to the single coil antenna, for the two-coil scenario, we can maximize the current by eliminating the reactance, i.e., $X + \omega M = 0$, and finally $(I_1 + I_2) = V/R_c = I_0$. When $X = -\omega M$, for TX_1 we have

$$R_c I_1 + \frac{\omega^2 M^2}{R_c^2 + \omega^2 M^2} R_c I_1 - j\omega M I_1 + \frac{\omega^2 M^2}{R_c^2 + \omega^2 M^2} j\omega M I_1 = V. \tag{6}$$

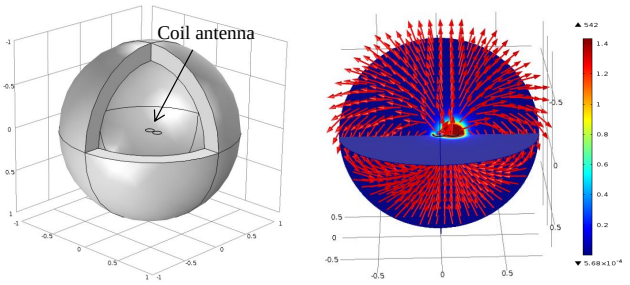

(a) FEM simulation model (b) Magnetic field intensity

Fig. 3. Simulation model and magnetic field distribution.

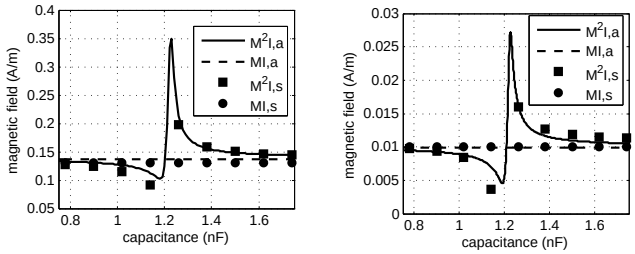

(a) 0.2m (b) 0.5m

Fig. 4. Effect of capacitor on radiated magnetic field. s stands for simulation results and a stands for analytical results.

Since R_c stands for the loss of metamaterial [11], we consider an optimal condition where $R_c << \omega^2 M^2$. Then, we can obtain $I_1 = V/(2R_c) = I_0/2$. Also, we can find that $I_2 = I_1$. For TX_1, the input power becomes $P_i = 1/4|I_0 V| = 1/2 P_{i0}$. However, the total radiation power is still the same since the radiation resistance does not change and $I_1 + I_2 = I_0$, as shown in (3). In other words, with less input power, we achieve the same radiated field intensity. Consequently, the this equivalent coil has higher efficiency. It should be noted that the resonance condition is

$$X = -\omega M, \quad C_a = \frac{1}{\omega^2 (M + L_c)}. \tag{7}$$

When C_a is fixed, there is only one resonant frequency. On the other hand, if we fix the resonant frequency, the optimal C_a is only one. In next section, we will show how to achieve multiple resonant frequencies.

1) Physical Interpretation of MI MIMO Enhancement: The increased radiation efficiency can be interpreted in an intuitive way. First and foremost, the resonant condition of the antenna array is $X + \omega M = 0$. For coaxial coils $M > 0$, since the radial magnetic field radiated by the antenna has the same direction as the small coils' orientation. In contrast, for coplanar coils $M < 0$, because the incoming field's direction and the passive coil's orientation is opposite. Originally, TX_2's resonant frequency is achieved when $X = \omega_0 L_c - \frac{1}{\omega_0 C_2} 0$. Now, since $M < 0$ the antenna array's resonant frequency shifts to a higher frequency ω_h. From the perspective of TX_2, at frequency ω_h, its reactance without coupling is $X = \omega_h L_c - \frac{1}{\omega_h C_2} > 0$. Since inductor's reactance is larger than 0, from (2) we have $XI_2 = -\omega_h M I_1$ and hence I_2 has the same sign as I_1, in other words the magnetic field radiated by TX_2 has the same direction as that by TX_1 which can help TX_1's radiation. However, if $X < 0$, this enhancement vanishes.

This enhancement has the same physical principle as the metamaterial-inspired small antennas [11], [12], [13] and M^2I [4], [5]. The passive coil antenna can be regarded as a kind of metamaterial which can enlarge the active coil antenna's radiation resistance and thus its efficiency. As stated in [11], this metamaterial is a kind of matching. In general, when TX_1 radiates signals at ω_h, the passive TX_2 can provide support which in turns increases the radiation efficiency of the antenna array.

2) Performance Evaluation: To validate the preceding results, we resort to numerical analysis and FEM simulation in COMSOL Multiphysics. In the numerical calculation, the radiation resistance, wire resistance, self-inductance, and the radiated magnetic field by a loop antenna can be found in [10, Ch. 5] and the mutual inductance between two coils is provided in [5]. The geometric structure of FEM simulation is depicted in Fig. 3(a) and the simulated magnetic field is shown in Fig. 3(b). Here, the coil is 5 cm in radius and it has 1 turn. The copper wire is 2 mm in radius. The operating frequency is 10 MHz and the environmental parameters: permeability, permittivity, and conductivity are set as $\mu_0 = 4\pi \times 10^{-7}$ H/m, $\epsilon_0 = 8.854 \times 10^{-12}$ F/m and 0, respectively.

Next, we compare the radiation efficiency of single input MI MIMO with a single coil; they have exactly the same configuration. Both of them are provided with 1 A current, i.e., $I_0 = I_1 = 1$; similar method was also adopted in [14]. Then, we gradually change the capacitor from 0.8 nF to 1.7 nF to find the resonant point. Since the square of magnetic field is proportional to radiation power, we use magnetic field intensity as a metric. In Fig. 4, we measure the magnetic field at 0.2 m and 0.5 m from the antenna to show this gain does not change with distance. Observe that, the coil antenna array is resonant when the capacitor is 1.2 nF. As predicted, when capacitor is small, the impedance of TX_2 is negative and its current has opposite direction as TX_1's. As the capacitor's value increases, $\omega L_c - 1/(\omega C) > 0$ which validates our conclusion that X should be larger than 0 to achieve resonance. Note that, for the single MI coil situation, since it has a constant 1 A current, its performance does not change with capacitor. The results imply that the magnetic field gain of MI MIMO over single coil can be as large as 2 times.

B. Multiple Input Transmitting Antenna Array

In this subsection, the single input system with single resonant frequency is extended to multiple input system to achieve multiple resonant frequencies. Note that, in (1) and (2), X_1 is not necessary to be the same as X_2. From (2) we can obtain $I_2 \approx -\omega M I_1 / X_2$. Since $M < 0$, X_2 should be larger than 0 so as to let I_2 have the same sign as I_1. Eliminating the reactance in (1), we can obtain the resonant condition $X_1 X_2 = \omega^2 M^2$. As we can see $X_1 = X_2 = -\omega M$ is just a special case.

Next, let us expand the resonance condition, which is

$$X_1 \cdot X_2 = (\omega L_c - \frac{1}{\omega C_1}) \cdot (\omega L_c - \frac{1}{\omega C_2}) = \omega^2 M^2. \tag{8}$$

Based on the above equation, we first discuss what was happened when $C_1 = C_2$ in last section. We consider C_1

and C_2 are known and ω is a variable; our target is the resonant frequency. As we can see, there are two meaningful solutions to the equation; the other two are negative which were dropped. When $C_1 = C_2 = C_a$ the first solution is (7) which have been discussed. The second solution is

$$\omega = \sqrt{\frac{1}{C_a(L_c - M)}}. \tag{9}$$

However, in previous section, we did not obtain this solution. The reason is that our preceding analysis is based on the condition that X_1 and X_2 both are positive. It is also possible that both of them are negative, in which way we can obtain the second solution. In such circumference, I_1 and I_2 have similar magnitude but opposite direction and thus they mutually cancel each other. As a result, the antenna array has very low efficiency and this is not a positive resonance. Therefore, we drop this solution.

Next, we consider $C_1 \neq C_2$, and we still have two solutions which are

$$\omega_1 = \sqrt{\frac{C_1L_c + C_2L_c - \sqrt{(C_1L_c - C_2L_c)^2 + 4C_1C_2M^2}}{2C_1C_2(L_c^2 - M^2)}}; \tag{10a}$$

$$\omega_2 = \sqrt{\frac{C_1L_c + C_2L_c + \sqrt{(C_1L_c - C_2L_c)^2 + 4C_1C_2M^2}}{2C_1C_2(L_c^2 - M^2)}}. \tag{10b}$$

Here we implicitly assume the resistance is negligible. Similarly, the larger one of them ω_2 can let both X_1 and X_2 be positive and the radiation efficiency can be improved as before. However, this time we pay special attention to the lower frequency ω_1 where both X_1 and X_2 are negative. Although we have found that this resonance leads to low efficiency, let us see what is the best performance we can achieve under this situation.

Inspecting (1) and (2), we can obtain $I_2 \approx -\omega MI_1/X_2$. Since both M and X_2 are negative, I_2 and I_1 have opposite direction. With the resonant condition (8) in mind, we can freely change X_1 and X_2. If we make X_2 extremely large, $I_2 \approx 0$, by which means we get rid of the negative effect and only keep I_1. The result is equivalent to the scenario where there is only TX_1. Consequently, we obtain two resonances: one is an enhanced resonance at the higher frequency, and the other one is a normal resonance at the lower frequency. Note that, X_2 can be changed by adjusting C_2. However, since the solution to (8) is also determined by C_2, we need to jointly design the resonance frequent and the resonance strength.

So far the antenna array is still fed from TX_1. Since impedance matching only works at a single frequency band, it is a great challenge to feed the antenna array from TX_1 at both the higher frequency and lower frequency. In order to address this problem, we can feed the higher frequency signal from TX_1 and match its impedance at that frequency. Similarly, we can feed the lower frequency signal from TX_2 and match it accordingly. The requirement is that at higher frequency both TX_1's and TX_2's reactance are positive and at the lower frequency TX_1's absolute reactance is as large as possible.

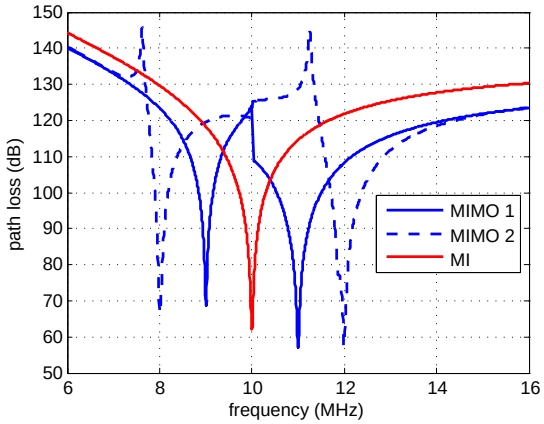

Fig. 5. 2×2 resonant frequency comparison with original MI. MIMO 1 achieves resonance at 9 MHz and 11 MHz; MIMO 2 achieves resonance at 8 MHz and 12 MHz.

C. Receiving Antenna Array

The receiving antenna array has the same configuration as the transmitting antenna array so as to make the system reciprocal. Due to the deep-subwavelength antenna interval and antenna size, the magnetic field intensity H_r at the two receiving antenna can be considered as the same. Then we can obtain

$$R_cI_1 + jX_1I_1 + j\omega MI_2 = V_r; \tag{11a}$$

$$R_cI_2 + jX_2I_2 + j\omega MI_1 = V_r, \tag{11b}$$

where $V_r = j\omega n\pi a^2\mu H_r$ [10]. With out loss of generality, we find the relation between I_1 and V_r by using (11),

$$\left[R_c + \frac{\omega^2M^2}{R_c^2 + X_2^2}R_c + j\left(X_1 - \frac{\omega^2M^2}{R_c^2 + X_2^2}X_2\right)\right]I_1 = \left[\left(1 - \frac{\omega MX_2}{R_c^2 + X_2^2}\right) - j\frac{\omega MR_c}{R_c^2 + X_2^2}\right]V_r. \tag{12}$$

To obtain a large current I_1, we need to let $\left(X_1 - \frac{\omega^2M^2}{R_c^2+X_2^2}X_2\right) = 0$. Similarly, if we consider R_c is small enough, we can obtain the same resonance condition as (8). As a result, the receiving antenna array has the same resonance frequency as the transmitting antenna array.

D. Dual Channel MI MIMO: Numerical Analysis

Before we proceed to discuss the channel performance, the resonant strength, i.e., path loss, is defined here. When the antenna array has N transmitting antennas and N receiving antennas, its overall path loss can be written as

$$\mathcal{L}(d, \omega) = \frac{\sum_{i=1}^{N} P_r^i}{P_{in}} = \frac{R_L \sum_{i=1}^{N} |I_r^i|^2}{V^2/|Z_t|}, \tag{13}$$

where P_r^i is the received power in receiving coil i, P_{in} is the input power, I_r^i is the current in receiving coil i (after impedance matching), and Z_t is the impedance of the transmitting coil at frequency ω. Note that, due to the non-perfect impedance matching, we consider the total input power to the system rather than the radiated power.

In Fig. 5, we compare a 2×2 antenna array with a 1×1 MI antenna. In the first MIMO configuration, C_1 is 210 pF and C_2 is 300 pF, and the resonance frequency is 9 MHz and 11 MHz. In the second MIMO configuration, C_1 is 174 pF and C_2 is 378 pF, and the resonance frequency is 8 MHz and 12 MHz. The coil antenna interval is 11 cm and the antenna radius is 5 cm. The distance between transmitting antenna and receiving antenna is 5 m. All other parameters are the same as previous discussion. Observe that, the higher-frequency resonance has lower path loss than MI which is due to the metamaterial enhancement. Secondly, as the difference between C_1 and C_2 increases, the second resonance at lower frequency becomes stronger. This is because at the lower resonant frequency, the impedance of TX_1 and TX_2 becomes drastically different. As a result, TX_1's current is very small and only TX_2 is transmitting. On the contrary, if $C_1 \approx C_2$, the resonance at the lower frequency will disappear and results in a single-resonance antenna array which has been discussed in preceding single-input transmitting antenna array.

III. N×N Antenna Array Design

The 2×2 coil antenna array is a simple example to provide insightful guidelines. In this section, we extend the results to a N×N antenna array. We consider N is a square number, i.e., 4, 9, 25,$\cdots$, in this way the antennas can be aligned in square girds. The coils' self-inductance is still L_c. Without loss of generality, we assume the capacitor in each coil is $C_1 < C_2 < C_3 < \cdots < C_N$. As a result, at any frequency ω, $X_1 < X_2 < X_3 < \cdots < X_N$. Also, the self-resonance frequency of each coil is $\omega_1 > \omega_2 > \omega_3 \cdots > \omega_N$.

Due to the reciprocal of the antenna array, here we consider the the receiver side of the $N\times N$ antenna array, which is simple to show the resonant condition,

$$\left[\left(R_i + \sum_{e=1,e\neq i}^{N} \frac{\omega^2 M_{ie}^2}{R_e^2 + X_e^2} R_e\right) + j\left(X_i - \sum_{e=1,e\neq i}^{N} \frac{\omega^2 M_{ie}^2}{R_e^2 + X_e^2} X_e\right)\right] I_i = \left[\left(1 - \sum_{e=1,e\neq}^{N} \frac{\omega M_{ie} X_e}{R_e^2 + X_e^2}\right) - j \sum_{e=1,e\neq i}^{N} \frac{\omega M_{ie} R_e}{R_e^2 + X_e^2}\right] V_r. \tag{14}$$

R_e consists of the coil resistance and real part of the reflected impedance from other coils. Similarly, X_2 consists of the coil reactance along with the imaginary part of the reflected impedance from other coils. Note that, the reflected resistance and reactance are high order functions of ω. Similar as preceding discussions, to achieve resonance the reactance on the left-hand side of (14) need to be zero. A closed-form solution is hard to derive due to the complexity. However, based on the 2×2 analysis, the performance is still predictable. Since different applications require different resonant frequencies, we provide an algorithms to freely achieve them.

The algorithm relies on the following two observations from the 2×2 antenna array. First, the highest resonance frequency is a little larger than ω_1. The reason is that, as discussed in previous section, X_2 is much larger than X_1 since the higher resonant frequency is much larger than TX_2's resonant frequency. To satisfy the resonance condition (8), $X_1 = \omega L_c - 1/(\omega C_1)$ should be small and the highest resonant frequency of the antenna array should be similar as the resonant frequency of TX_1. Moreover, the second, third, $\cdots$, N^{th} resonance frequency of the antenna array should be a little smaller than ω_2, ω_3, $\cdots$, ω_N, respectively. From the 2×2 array we learn that the non-enhanced resonance is because of the negative reactance. To make X_2 negative, we need the frequency to be smaller than ω_2 (coil 2's self-resonance frequency). Due to the inherent property of reactance, slightly change the frequency can lead to large reactance. Therefore, the resonant frequency should be around the coil's own resonant frequency and also a little smaller than it.

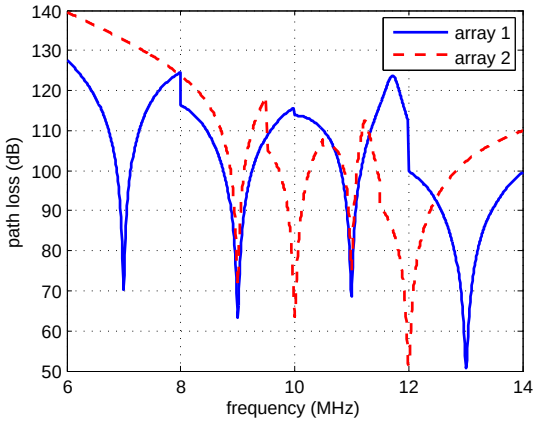

Fig. 6. 4×4 array resonant frequency. Resonant frequency of array 1: 7,9,11,13 (MHz); resonant frequency of array 2: 9,10,11,12 (MHz).

The second observation is that the frequency interval between each pair of resonant frequencies can be changed by adjusting mutual inductances, as suggested by (10). The mutual inductance can be adjusted by changing coil turns, size, mutual interval, orientation, among others. Referring back to (10), the difference between ω_1 and ω_2 is determined by C_1, C_2 and M. Originally, when C_1 is similar as C_2 we can expect the two resonant frequencies should be very close. However, due to the large mutual inductance between them, this frequency interval cannot be 0, i.e., the higher and lower resonant frequency cannot be the same. In contrast, if we have small mutual inductance, we can have very close resonant frequencies by letting C_1 and C_2 be similar.

Based on the above observations, we provide the following heuristic method to design the resonant frequency. In this method, we first set the capacitors to let each coil resonant at the objective resonance frequency. Then, from the highest resonance frequency, we change the capacitor in coil 1 from C_N to $1.5C_N$. Since the array's highest resonance frequency is larger than coil N's resonant frequency, the capacitance should gradually increase to decrease its own resonant frequency which in turn increases the antenna array's highest resonant frequency. For other capacitors, they should change from lower value to achieve negative reactance. If we cannot find the optimal capacitance to make the coil array resonant at the objective frequency, which means the coils are too close and their mutual inductances are too large. Hence, we increase their mutual interval to do another round search until we can obtain the optimal capacitor.

Next, by using a 4×4 antenna array, we try to design its

resonant frequency to achieve 4 wireless channels. In this scenario, the antennas are placed in a square grid. We try to design the antenna array to let it first be resonant at 7, 9, 11, and 13 MHz. Then, we consider a even more compact resonant frequencies, 9, 10, 11, and 12 MHz. From the results we can see the strongest resonance still happens at the highest resonant frequency and the path loss is even lower than a 2×2 antenna array. Also, to achieve close resonant frequencies, we need to increase the antenna interval to reduce their mutual inductance.

IV. Resource Allocation and Channel Capacity Analysis

So far, we have designed multiple channel MI MIMO antenna array. As we have seen, multi-band MI MIMO is different from existing MIMO systems; the multiple antennas are utilized to create multiple resonances rather than providing more diversities. Therefore, its enhancement, i.e., channel capacity gain, need to be reevaluated. In this section, we first analyze the gain theoretically which is followed by numerical analysis.

The wireless channel of a N×N antenna array can be described by a N×N diagonal matrix **H**. Element h_{ij} denotes the signal transmitted by antenna i and then received by antenna j. **H** is a diagonal matrix because of that different antennas resonant at different frequencies. There is only a pair of antennas in the transmitting and receiving array having the same frequency which is the diagonal element. In other words, in the receiving antenna array, only one antenna can efficiently receive the signal at its own resonant frequency, although other antennas can also receive the signal but the strength is very low due to the high impedance when the antenna is not resonant.

The channel capacity can be written as

$$C = \sum_{i=1}^{N} \mathcal{B}_i log\left(1 + \frac{P_i^t h_{ii}}{N_0}\right), \tag{15}$$

where $\mathcal{B}_i$ is the bandwidth of the i^{th} channel, P_i^t is the transmission power allocated to the i^{th} channel and N_0 is the noise density. At high SNR regime, it is optimal to allocate power to each of the channel and, therefore, the gain can approximated by N. At the low SNR regime, it is optimal to allocate all the power to the best channel which is the highest-frequency channel with metamaterial-inspired enhancement. As a result, the gain is only from the metamaterial-inspired enhancement.

The multiple-resonance channel can be considered as a frequency-selective channel and we resort to water-filling [15] to allocate the power. The 2×2 antenna array resonant at 8 MHz and 12 MHz, and the 4×4 antenna array resonant at 7 MHz, 9 MHz, 11 MHz and 13 MHz, are utilized to show the channel capacity improvement in comparison with the original MI. The antenna input power is 1 dBm and the signal is distorted by the high noise and low noise whose power density are -114 dBm and -154 dBm, respectively. The 3-dB bandwidth is considered. The results are shown in Fig. 7 and we have the follow two primary observations. First, when the noise is low, i.e., SNR is large or distance is small, the 4×4 antenna array can achieve the highest data rate and the gain is also linear with the antenna number. For instance, the

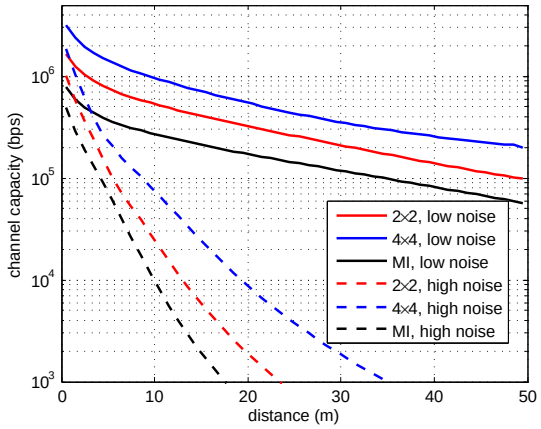

Fig. 7. Channel capacity of MI MIMO and original MI.

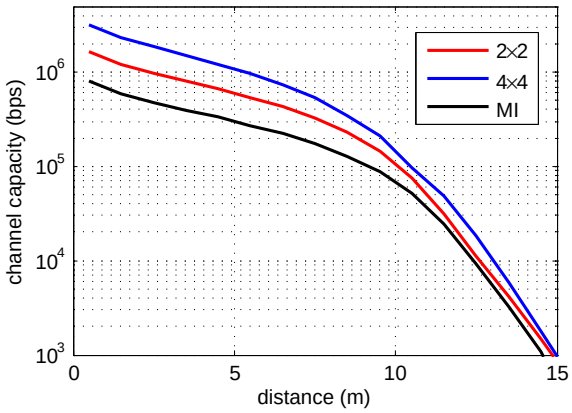

Fig. 8. Channel capacity in lossy medium; conductivity of the medium is 0.005 S/m.

gain of 2×2 antenna array over original MI and the gain of 4×4 antenna array over 2×2 antenna array is almost the same. Therefore, at high SNR, the more antennas, the large channel number and we can achieve more gain. At low SNR, i.e., high noise or long distance, the metamaterial-inspired gain is much more significant than antenna gain. This is because when SNR is low only the best channel is utilized. Thanks to the enhancement at the highest resonant frequency, this channel is much better than the original MI. Also, the more antennas, this channel has more supporters to increase the radiating antenna's efficiency and thus the stronger the channel gain. As a result, the 4×4 antenna array has even larger gain when the SNR is low.

M^2I was proposed to enable wireless communication in complex and lossy medium [4]. Here, we consider that the medium is lossy with conductivity 0.005 S/m. This will lead to higher coil resistance and slightly smaller self-inductance [3]. In our previous analysis, we implicitly assume R_c is negligible. However, as the medium becomes lossy, the coil resistance increases due to the reflected impedance from the environment and thus R_c cannot be neglected. In addition, due to the lossy medium, the signal experiences higher absorption. As a result, although we consider the same antenna input power and noise density, the SNR drastically deceased. Next, we consider the low noise and plot channel capacity for each antenna array in

Fig. 8. Observe that to achieve as low as 1 kbps data rate, the communication range should be within 15 m which is much smaller than without loss. Although the 4×4 antenna array still achieves the best channel capacity, we can see the gain gradually reduces as the distance increases. This is because of that in the near region, i.e., within 7 m, the gain is because of the channel number; the more antennas, the larger the gain. However, in the far region, the dominant channel becomes the metamaterial-enhanced channel. Due to the larger R_c, those passive coil antennas becomes inefficient which is equivalent to the high loss metamaterial [4]. As a result, the gain becomes much smaller than the channel number gain.

V. Conclusion

Magnetic Induction (MI) wireless communication has been extensively adopted in complex environments. Its communication range is significantly improved by M^{2}I. However, MI only has one resonant frequency and its bandwidth is narrow which make it hard to be applied in wireless networks. In this paper, a MI MIMO antenna array is proposed to create multiple channels to increase MI communication's overall bandwidth. The near field antenna coupling is rigorously modeled and analyzed. By using metamaterial-inspired antenna design technique, we obtain an enhanced channel in conjunction with multiple original MI channels. An algorithm is proposed to find the optimal capacitor in each coil to make the antenna array operate at the desired frequency band efficiently. Through numerical analysis, we show that the multi-channel MI MIMO can significantly increase the channel capacity. Besides increasing the channel capacity, multiple-channel MI MIMO can also be utilized in many other applications, such as reducing interference and improving network capacity in wireless networks, enable simultaneous wireless communication and wireless power transfer by using different channels, among others.

Acknowledgement

This work was supported by US National Science Foundation (NSF) under Grant Number 1547908.

References

[1] Z. Sun and I. F. Akyildiz, "Magnetic induction communications for wireless underground sensor networks," *Antennas and Propagation, IEEE Transactions on*, vol. 58, no. 7, pp. 2426–2435, 2010.

[2] I. F. Akyildiz, P. Wang, and Z. Sun, "Realizing underwater communication through magnetic induction," *Communications Magazine, IEEE*, vol. 53, no. 11, pp. 42–48, 2015.

[3] H. Guo, Z. Sun, and P. Wang, "Channel modeling of MI underwater communication using tri-directional coil antenna," in *2015 IEEE Global Communications Conference (GLOBECOM)*, San Diego, CA, Dec 2015.

[4] H. Guo, Z. Sun, J. Sun, and N. M. Litchinitser, "M^{2}I: Channel modeling for metamaterial-enhanced magnetic induction communications," *Antennas and Propagation, IEEE Transactions on*, vol. 63, no. 11, pp. 5072–5087, 2015.

[5] H. Guo and Z. Sun, "M^{2}I communication: From theoretical modeling to practical design," in *2016 IEEE International Conference on Communications (ICC)*, Kuala Lumpur, Malaysia, May 2016. [Online]. Available: arXiv:1510.08466[physics.ins-det]

[6] X. Tan, Z. Sun, and I. F. Akyildiz, "A testbed of magnetic induction-based communication system for underground applications," *IEEE Antennas and Propagation Magazine*, 2015.

[7] R. Janaswamy, "Effect of element mutual coupling on the capacity of fixed length linear arrays," *Antennas and Wireless Propagation Letters, IEEE*, vol. 1, no. 1, pp. 157–160, 2002.

[8] B. Clerckx, C. Craeye, D. Vanhoenacker-Janvier, and C. Oestges, "Impact of antenna coupling on 2× 2 mimo communications," *Vehicular Technology, IEEE Transactions on*, vol. 56, no. 3, pp. 1009–1018, 2007.

[9] H. J. Kim, J. Park, K. S. Oh, J. P. Choi, J. E. Jang, and J. W. Choi, "Near-field magnetic induction mimo communication using heterogeneous multi-pole loop antenna array for higher data rate transmission," *IEEE Transactions on Antennas and Propagation*, vol. PP, no. 99, pp. 1–1, 2016.

[10] C. A. Balanis, *Antenna theory: analysis and design*. John Wiley & Sons, 2005, vol. 1.

[11] N. Engheta and R. W. Ziolkowski, *Metamaterials: Physics and Engineering Explorations*. John Wiley Publishing Company, 2006.

[12] A. Erentok and R. W. Ziolkowski, "Metamaterial-inspired efficient electrically small antennas," *Antennas and Propagation, IEEE Transactions on*, vol. 56, no. 3, pp. 691–707, 2008.

[13] R. W. Ziolkowski and A. Erentok, "At and below the chu limit: passive and active broad bandwidth metamaterial-based electrically small antennas," *IET Microwave, Antennas and Propagation*, vol. 1, no. 1, 2007.

[14] R. W. Ziolkowski and A. D. Kipple, "Application of double negative materials to increase the power radiated by electrically small antennas," *IEEE Transactiions on Antenna and Propagation*, vol. 51, no. 10, pp. 2626–2640, 2003.

[15] D. Tse and P. Viswanath, *Fundamentals of wireless communication*. Cambridge university press, 2005.